REVISTA INTERDISCIPLINAR DE PESQUISA EM ENGENHARIA

CILAMCE 2016
XXXVII IBERIAN LATIN AMERICAN CONGRESS ON COMPUTATIONAL METHODS IN ENGINEERING
BRASÍLIA - DF - BRAZIL

A STUDY OF THE ROLLING LOAD CALCULATION MODELS FOR FLAT COLD ROLLING PROCESS

Hugo L. F. Nascimento

Yukio Shigaki

Sandro C. Santos

Alexandre Z. Hubinger

hugoleo_junior@hotmail.com

yukio@des.cefetmg.br

sandro@des.cefetmg.br

hubinger@des.cefetmg.br

Federal Centre of Technological Education of Minas Gerais (CEFET-MG)

Amazonas avenue, 7675 - Campus II, - CEP 30510-000 - Belo Horizonte/MG, Brazil

Jánes L. Júnior

janes@pucminas.br

Pontifícia Universidade Católica - MG

Dom José Gaspar avenue, 500 - CEP 30535-901 - Belo Horizonte/MG, Brazil

Abstract. *In order to keep the rolling products free of defects, the calculation and constant assessment of the rolling load and torque are required. Many theories for rolling load calculation were developed and among them the most used nowadays still are the Bland and Ford 's (1948) model and Alexander's (1971) model in order to achieve a better online control for reversible and tandem cold rolling mills. In this work those models were implemented in a numerical calculation software. The elastic roll's deformation was taken into account using the Hitchcock´s formula for the deformed roll radius in an iterative way. Those models state that the friction hill (or normal pressure) in the contact arc keeps circular after the elastic deformation. This hypothesis is analysed with a third offline model for calculating the rolling load, named Noncirc (Shigaki et al., 2015), that considers the real roll elastic deformation (not circular anymore). Two cold rolling cases were considered and the*

friction coefficient was varied in order to evaluate the influence of this parameter on the calculated rolling load/width, the contact arc length and profile and pressure distribution over the contact arc. It was found that both models present imprecise results for both cases analysed, as the thickness is very low and the strip is very work hardened. The noncircular model shows higher loads and larger arc of contacts, but has the drawback of being offline.

Keywords: *Rolling load, Cold rolling, Friction hill, Noncircular arc.*

1 INTRODUCTION

Rolling is a metal forming process in which a material (sheet, plate, strip) is forced between two rotational rolls, in order to reduce its thickness. Depending on the equipment characteristics, it is possible to say that the rolling process presents good dimensional control and high productivity due to its continuity (Helman and Cetlin, 2005).

The rolling load calculation is a critical parameter when looking for the correct rolling mill setup in steel rolling. The rolling load distribution over the length of the contact arc between the sheet and rolls is a complicated phenomenon and it is affected by several factors as rolling temperature, rolls geometry, back and front tension, rolling speed, microstructural variations in the stock (which leads to variations in yield stress), etc. Modern roll gap setup and profile control need an accurate prediction of the roll load under different rolling conditions, what justifies the importance of the rolling load calculation (Yang et al., 2004).

The cold rolling process was taken as a research subject during many decades, currently some theories are capable of output a valuable and detailed description of the gap between the rolls during the rolling process (Grimble et al., 1978). First off Siebel (1925) and von Karman (1925) started the studies on the topic, their analysis introduced the vertical segments homogeneous compression concept of the sheet during the rolling. Other fundamental supposition was the occurrence of a neutral plane inside the length of the contact arc (Freshwater, 1996).

In addition, another approximation, which implies great simplification on the theories, is that the contact surface between roll and sheet remains circular, leading to an easier solution with minor errors. Among other suppositions, the friction coefficient was chosen as constant and the sheet and rolls elastic strain were neglected. However, for certain practical rolling conditions as in thin sheets rolling last stand, the algorithms based on the classical theory frequently fail to converge or present too discrepant values (Grimble et al., 1978).

The models proposed by Sims (1945) and Bland and Ford (1948) allowed the problem to be solved analytically, avoiding most of the numerical integrations, unlike the Orowan (1943) model, which is far more complex and demands more calculations. However, Bland and Ford simplifications led to a sacrifice in accuracy (Alexander, 1971).

Trying to reach greater precision in predicting rolling parameters Ford and his colleagues (Ford, Ellis and Bland, 1951; Lianis and Ford, 1956; Bland and Sims, 1953 apud Alexander, 1971) introduced the contribution of the elastic strain zones at the entry and exit of the contact arc and allowed for strain hardening using flow equations.

With the development of digital computational power, the complexity of differential equations that describes any physical phenomenon ceased to stand as barrier to find problem solutions, with this in mind Alexander (1972 apud Freshwater, 1996) proposed a comprehensive numerical solution to Orowan's model, although he did not take into account the inhomogeneity strain factor, as proposed by Orowan in his theory. Alexander used a fourth order Runge-Kutta routine to solve von Karman first order differential equation with certain boundary conditions.

Using a numerical calculation software, the Bland and Ford's model corrected with Hitchcock's deformed radius formula together with Alexander's model corrected with the Hitchcock's deformed radius formula modified by Ford (1951) were implemented. From this point, both models were compared testing various rolling parameters based on two steel rolling cases. Both models were also compared with a noncircular rolling model from Shigaki *et al* (2015).

2 STUDIED MODELS

2.1 Bland and Ford's model

Starting from von Karman's equation stated below Eq. 1 Bland and Ford (1948) suggested some simplifications in a way that the solution to this equation could be found analytically. Equation 1 is easily solved numerically, although its analytical solution may not be (Helman and Cetlin, 2005).

$$hS\frac{d\left(1-\frac{p}{S}\right)}{d\emptyset}+\left(1-\frac{p}{S}\right)\frac{d(hS)}{d\emptyset}=-p2R'(sen\emptyset\pm\mu cos\emptyset) \tag{1}$$

Von Karman's theory is based on the following assumptions:

- Plane strain state.
- Homogeneous strain in each vertical section.
- Constant friction coefficient (Coulomb friction).
- Circular contact arc (with deformed radius R').
- The existence of a neutral plane inside the contact arc.
- Elastic sheet and rolls strain is neglected.

Figure 1 helps to understand the meaning of the variables used.

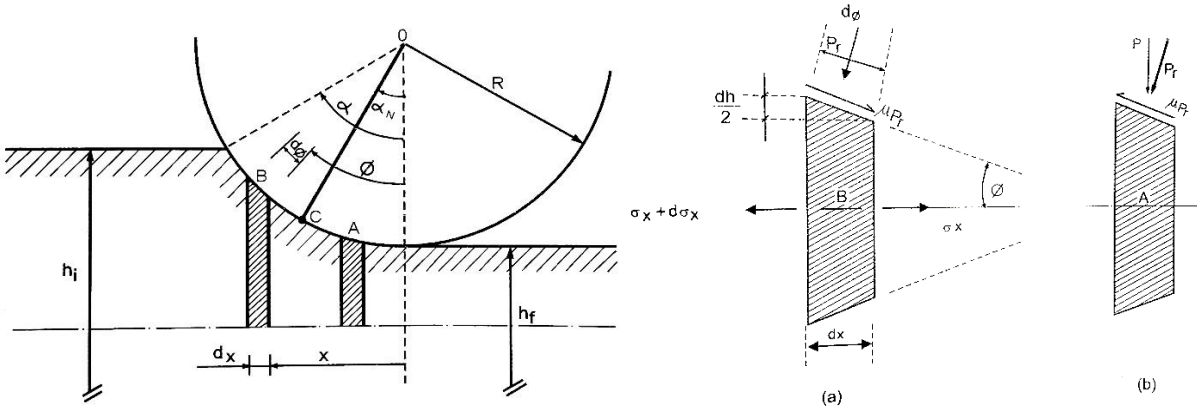

Figure 1 – Stress equilibrium analysis acting in the element A (a) e B (b).
Source: Adapted from Helman and Cetlin, 2005.

In equation (1):

- *h – sheet thickness along the contact arc.*
- *S – plane strain yield strength.*
- *p – roll vertical pressure, for small angles pr ≈ p.*
- *R' – deformed working roll radius.*
- *Ø – angular coordinate.*

In all equations cited in this paper the uppermost of any pair of algebraic signs refers to the exit side, the lower to the entry side of the neutral plane.

Because of the high stress applied to the rolls by the contact with the stock, they get locally flattened and have a different radius from its original. The first known author to develop a relationship concerning the roll radius and the deformed roll radius was Hitchcock (1935 apud Roberts, 1978), making use of Hertz's elastic bodies contact theory. His studies resulted in the following equation, which was used in this work at Bland and Ford's model:

$$R' = R\left[1 + \frac{c}{h_i - h_f}\left(\frac{P}{W}\right)\right] \tag{2}$$

Where P is the rolling load, W is the sheet width, R is the working roll radius and c is given by equation (3):

$$c = \frac{16\left(1-\nu_{roll}^2\right)}{\pi E_{roll}} \tag{3}$$

Where E_{roll} is the roll Young's modulus and ν_{roll} is the roll Poisson's coefficient.

When it comes to Bland and Ford's assumptions, they stated that in most rolling cases, the rolling pressure variation along the contact arc is bigger than the material yield strength variation. Also the hS product is yet smaller, in the sight that when S goes up, h goes down (Helman and Cetlin, 2005). Thus, evaluating equation 1 it is reasonable to say that:

$$hS\frac{d\left(1-\frac{p}{S}\right)}{d\emptyset} \gg \left(1-\frac{p}{S}\right)\frac{d(hS)}{d\emptyset}$$

However this becomes invalid whenever the material strain harden too fast, or the applied back tension is too high, because both this factors make $\frac{p}{S}$ variation along the contact arc to be smaller (Helman and Cetlin, 2005).

Therefore, equation 1 becomes:

$$hS\frac{d}{d\emptyset}\left(\frac{p}{S}\right) = 2R'p(sen\emptyset \pm \mu cos\emptyset) \tag{4}$$

The variable h is the sheet thickness along the contact arc, and it is given by equation 5 below.

$$h = h_f + 2R'(1 - cos\emptyset) \tag{5}$$

Using small angle approximations:

$$sen\,\emptyset \cong \emptyset \qquad \text{and} \qquad cos\emptyset \cong 1 - \frac{\emptyset^2}{2}$$

Equation 5 becomes:

$$h = h_f + 2R'(1 - cos\emptyset) \cong h_f + 2R'\frac{\emptyset^2}{2}$$

Thus, equation 4 becomes:

$$\frac{d}{d\emptyset}\left(\frac{p}{S}\right) = 2R'\frac{p}{S}\frac{\emptyset \pm \mu}{h_f + R'\emptyset^2} \rightarrow \frac{d(p/S)}{(p/S)} = \frac{2\emptyset d\emptyset}{\frac{h_f}{R'}+\emptyset^2} \pm \frac{2\mu d\emptyset}{\frac{h_f}{R'}+\emptyset^2} \tag{6}$$

Equation 6 is easily integrated and the solution is given by:

$$\ln(p/S) = \ln\left(\frac{h_f}{R'} + \emptyset^2\right) \pm 2\mu \frac{1}{\frac{\sqrt{h_f}}{R'}} arctg \frac{\emptyset}{\frac{\sqrt{h_f}}{R'}} + constant$$

Adopting:

$$H = 2\sqrt{\frac{R'}{h_f}} arctg\left(\sqrt{\frac{R'}{h_f}}\emptyset\right) \tag{7}$$

Results in:

$$\ln\frac{p}{S} = \ln\left(\frac{h}{R'}\right) \pm \mu H + constant$$

In another way:

$$\frac{p^+}{S} = C_1\frac{h}{R'}\exp(+\mu H) \qquad \text{Valid to the exit side} \tag{8}$$

$$\frac{p^-}{S} = C_2\frac{h}{R'}\exp(-\mu H) \qquad \text{Valid to the entry side} \tag{9}$$

When back and front tensions are applied equation 8 and 9 become:

$$\frac{p^+}{S} = \left(1 - \frac{T_f}{S_f}\right)\frac{h}{h_f}\exp(+\mu H) \qquad \text{Valid to the exit side} \tag{10}$$

$$\frac{p^-}{S} = \left(1 - \frac{T_i}{S_i}\right)\frac{h}{h_i}\exp(\mu(H_i - H) \qquad \text{Valid to the entry side} \tag{11}$$

In equations 10 and 11:

- T_f – *front applied tension.*
- T_i – *back applied tension.*
- S_f – *material plane strain yield strength at the exit side (see equation 17 to 20).*
- S_i – *material plane strain yield strength at the entry side (see equation 17 to 20).*
- h_f – *sheet thickness at exit.*
- h_i – *sheet thickness at entry.*
- H_i – *equation 7 (H) calculated when* $\emptyset = \alpha$.

The contact arc length is given by equation 12:

$$L = \sqrt{R^2 - \left(R - \frac{\Delta h}{2}\right)^2} = \sqrt{R\Delta h - \frac{\Delta h^2}{4}} \tag{12}$$

The contact angle can be written as follows:

$$sen\ \alpha = \frac{L}{R} = \frac{\sqrt{R\Delta h - \frac{\Delta h^2}{4}}}{R} \rightarrow \alpha = \text{asin}\left(\frac{\sqrt{R\Delta h - \frac{\Delta h^2}{4}}}{R}\right) \tag{13}$$

Equations 10 and 11 output the pressure distribution along the contact arc, thus in order to find the total pressure per sheet width the following integration is needed:

$$\frac{P}{w} = \int_0^L p dx$$

Usually dx is translated into angular coordinates, and for most cold rolling cases the following approximation is valid, because contact angles are small:

$$dx = R' d\emptyset cos\emptyset \approx R' d\emptyset \left(1 - \frac{\emptyset^2}{2}\right) \approx R' d\emptyset$$

Therefore:

$$\frac{P}{w} = \int_0^{\alpha} p(\emptyset) R' d\emptyset = R' \left(\int_0^{\alpha_N} p^+(\emptyset) d\emptyset + \int_{\alpha_N}^{\alpha} p^-(\emptyset) d\emptyset\right) \tag{14}$$

In equation 14:

- α – *is the contact angle.*
- α_N – *is the neutral plane angular coordinate.*

The value of α_N is found when:

$$p^+ = p^-$$

Solving the equality:

$$\alpha_N = \sqrt{\frac{h_f}{R'}} tan\left[\sqrt{\frac{h_f}{R'}} \frac{H_N}{2}\right] \tag{15}$$

And:

$$H_N = \frac{H_i}{2} - \frac{1}{2\mu} ln\left[\frac{h_i}{h_f} . \frac{\left(1 - \frac{T_f}{S_f}\right)}{\left(1 - \frac{T_i}{S_i}\right)}\right] \tag{16}$$

For the first iteration in the iteration process, the deformed radius (R') is replaced with the regular roll radius (R) at all equations. With the value for $\frac{P}{w}$ now calculated, it is then used in equation 2 to calculate the deformed roll radius. This new deformed roll radius is used to recalculate a new rolling load per unit width. The process is continued until the stop criterion is met.

In both Bland & Ford's and Alexander's models, the following flow equation was applied in order to include the strain hardening effect that the material undergoes:

$$\sigma = (AA + BA \times \bar{\varepsilon}) \times (1 - CA \times exp(-DA \times \bar{\varepsilon})) - EA \tag{17}$$

Where:

- σ – *material uniaxial yield stress.*
- $\bar{\varepsilon}$ – *uniaxial equivalent strain.*
- *AA, BA, CA, DA, EA – material related coefficients.*

The uniaxial equivalent or effective strain ($\bar{\varepsilon}$) in plane strain compression is given in terms of the true strain in equation 18 and 19 (Alexander, 1971):

$$\bar{\varepsilon} = \frac{2}{\sqrt{3}}\varepsilon \tag{18}$$

Where:

$$\varepsilon = ln\left(\frac{h_i}{h}\right) = ln\left(\frac{h_i}{h_f + 2R'(1-cos\emptyset)}\right) \tag{19}$$

In plane strain compression the yield stress is given by equation 20 (Alexander, 1971).

$$S = \frac{2}{\sqrt{3}}\sigma \tag{20}$$

2.2 Alexander's model

Making use of Orowan's approach, Alexander (1971) developed a FORTRAN algorithm that could solve most rolling problems efficiently. However, he neglected Orowan's inhomogeneity factors, which are mostly valid when the ratio between the contact arc length and the mean thickness is less than 3 $\left({}^{L}/_{h} < 3\right)$. In cold rolling is usual to have ${}^{L}/_{h} > 3$, therefore the homogeneous compression hypothesis is valid (Montmitonnet, 2006).

Alexander's model is flexible in a way that it could even be used for hot rolling conditions, needing only slight modifications in theory as shown by Chen et al (2014) in his article.

Ford et al. (1951) demonstrated how Hitchcock's equation should be modified in order to include the elastic strain effect that occurs at the entry and exit of the roll bite, keeping the contact arc as a circular surface, what is shown in equations 21 to 26:

$$R' = R\left[1 + \frac{c}{\left(\sqrt{\Delta h + \delta_{ef} + \delta_t} + \sqrt{\delta_{ef}}\right)^2}(P)\right] \tag{21}$$

$$\Delta h = h_i - h_f \tag{22}$$

$$\delta_{ef} = \frac{(1-v_{sheet}^2)(S_f - t_{ef})h_f}{E_{sheet}} \tag{23}$$

$$t_{ef} = T_f - \frac{2\mu P_{ef}}{h_f} \tag{24}$$

$$P_{ef} = \frac{2}{3}\sqrt{\frac{R'(1-v_{sheet}^2)h_f}{E_{sheet}}}\left(S_f - t_{ef}\right)^{\frac{3}{2}} \tag{25}$$

$$\delta_t = \frac{\nu_{sheet}(1+\nu_{sheet})(h_f T_f - h_i T_i)}{E_{sheet}} \tag{26}$$

In the equations above the undefined variables have the following meaning:

- ν_{sheet} – *rolling material Poisson's coefficient.*
- E_{sheet} – *rolling material Young's modulus.*

In Alexander's (1971) work it is shown that t_{ef} e P_{ef} must be iteratively found, since they depend on each other. For the first iteration the deformed radius at P_{ef} equation can be estimated with the basic Hitchcock's formula and $t_{ef} = T_f$.

Following Orowan's method, Alexander's model easily deals with the mixed boundary conditions (slip/no-slip regions) in the roll bite. This is introduced in the codding with the following statement: solve the shear stress (τ_s) using $\tau_s = \mu p_r$ and $\tau_s = K = S/2$, and use whichever is the smaller (Alexander, 1971). A slip zone will occur if the shear stress is smaller than the material shear strength, and a no-slip/sticking zone will take place if the shear stress reaches the material shear strength. For the slip zone, the shear stress is given by the Coulomb's friction law, which means it is the product between the roll normal pressure (p_r) and the friction coefficient (μ). For the no-slip region the shear stress can never be higher than the material shear strength which is K=$S/2$ (Alexander, 1971).

Alexander (1971) considered von Karman's basic equation under the following format:

$$\frac{d[h(p_r - S \mp \tau_s tan\emptyset)]}{d\emptyset} = 2R'(p_r sen\emptyset \pm \tau_s cos\emptyset) \tag{27}$$

In equation (27) the upper algebraic signs refer to the situation on the exit side of the neutral plane, the lower to the entry side. Figure 2 refers to some variables used.

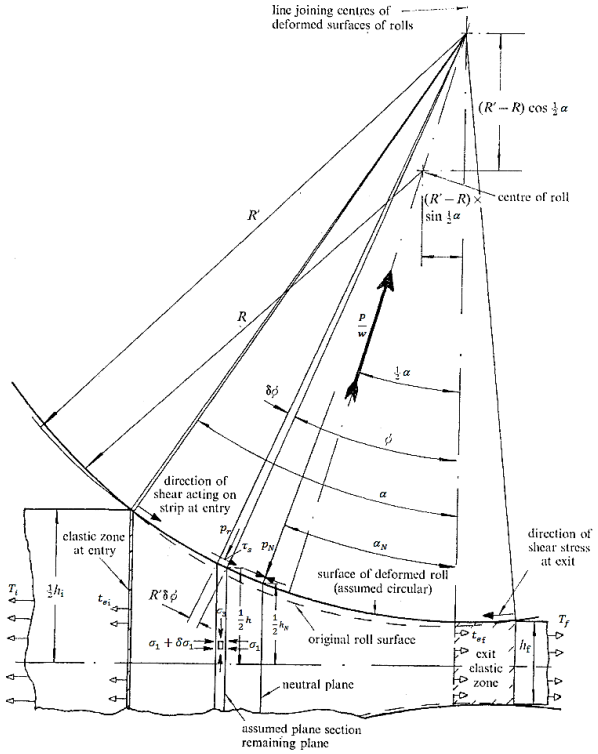

Figure 2 – Detailed geometry and variables.
Source: Adapted from Alexander, (1971).

At figure 2:

- $\frac{P}{w}$ – *pressure per sheet width.*
- t_{ei} – *back tension stress actually applied to the plastic arc.*
- t_{ef} – *front tension stress actually applied to the plastic arc.*

Slip zone. Using $\boldsymbol{\tau_s = \mu p_r}$ in equation 27 the following differential equation is encountered:

$$\frac{dp_r}{d\emptyset} = g_{1(\emptyset)} p_r + g_{2(\emptyset)} \tag{28}$$

Where:

$$g_{1(\emptyset)} = \frac{\pm \mu sec\emptyset \left(\frac{2R'}{h} + sec\emptyset\right)}{(1 \mp \mu tan\emptyset)} \tag{29}$$

$$g_{2(\emptyset)} = \frac{\left(\frac{2R'S}{h} sen\emptyset + \frac{dS}{d\emptyset}\right)}{(1 \mp \mu tan\emptyset)} \tag{30}$$

No-Slip/Sticking zone. Using $\boldsymbol{\tau_s = \frac{S}{2}}$ in equation 27 the following is found:

$$\frac{dp_r}{d\emptyset} = g_{\mathbf{3}(\emptyset)} \tag{31}$$

Where:

$$g_{3(\emptyset)} = S\left\{\frac{2R'}{h} sen\emptyset \left(1 \pm \frac{1}{2} tan\emptyset\right) \pm \left(\frac{R'}{h} cos\emptyset + \frac{1}{2} sec^2\emptyset\right)\right\} + \left(1 \pm \frac{1}{2} tan\emptyset\right) \frac{dS}{d\emptyset} \tag{32}$$

Again, the upper algebraic signs refer to the situation on the exit side of the neutral plane, the lower to the entry side (Alexander, 1971).

Boundary conditions. In the plastic deformation zone, the boundary conditions are determined from the equilibrium equation for a volume finite element, as shown in figure 2, which means:

$$\sigma_3 R'\delta\emptyset cos\emptyset = p_r R'\delta\emptyset cos\emptyset \mp \tau_s R'\delta\emptyset sen\emptyset \quad \text{or} \quad \sigma_3 = p_r \mp \tau_s tan\emptyset \tag{33}$$

The upper algebraic signs refer to the exit side, the lower to the entry side (Alexander, 1971).

The compressive vertical and horizontal stress can be related using the Huber-Mises yield criterion:

$$\sigma_3 - \sigma_1 = 2K = S \rightarrow \sigma_3 = S + \sigma_1 \tag{34}$$

Thus, replacing equation 34 in equation 33:

$$\sigma_1 = p_r - S \mp \tau_s tan\emptyset \tag{35}$$

Therefore, at the entry of the plastic arc, when $\emptyset = \alpha$, $S = S_i \; e \; \sigma_1 = -t_{ei}$, the roll normal pressure is:

$$p_{ri} = S_i - t_{ei} - \tau_{si} tan\alpha \tag{36}$$

Or:

$$p_{ri} = (S_i - t_{ei})/(1 + \mu tan\alpha) \quad \text{if} \quad \tau_{si} = \mu p_{ri} \tag{37}$$

$$t_{ei} = T_i - \frac{2\mu P_{ei}}{h_i} \tag{38}$$

$$P_{ei} = \frac{(1-\nu^2)h_i}{4} \frac{(S_i - t_{ei})^2}{E} \sqrt{\frac{R'}{h_i - h_f}} \tag{39}$$

At the exit, where $\emptyset = 0$:

$$p_{rf} = S_f - t_{ef} \tag{40}$$

$$t_{ef} = T_f - \frac{2\mu P_{ef}}{h_f} \tag{41}$$

$$P_{ef} = \frac{2}{3} \sqrt{\frac{R'(1-\nu^2)h_f}{E}} \left(S_f - t_{ef}\right)^{\frac{3}{2}} \tag{42}$$

As shown earlier in this work, (t_{ei},P_{ei}) and (t_{ef},P_{ef}) must be iteratively found, since they depend on each other. For the first iteration the deformed radius at P_{ei} and P_{ef} equations can be estimated with the basic Hitchcock's formula and $t_{ei} = T_i$, $t_{ef} = T_f$ should be used.

Calculating the roll force per unit width. Alexander assumed that the roll force per unit width $\left(\frac{\boldsymbol{P}}{\boldsymbol{w}}\right)$ must act midway along the angular arc of contact and be directed towards the deformed roll center. Considering this, the rolling load is written as a function of the projected $\boldsymbol{p_r}$ e $\boldsymbol{\tau_s}$ in this direction (Alexander, 1971):

$$\frac{P}{w} = R' \int_0^{\alpha} p_r \cos\left(\emptyset - \frac{1}{2}\alpha\right) d\emptyset + R' \left[\int_{\alpha_N}^{\alpha} \tau_s sen\left(\emptyset - \frac{1}{2}\alpha\right) d\emptyset - \int_0^{\alpha_N} \tau_s sen\left(\emptyset - \frac{1}{2}\alpha\right) d\emptyset\right] \tag{43}$$

Therefore, the total rolling load per unit width (P) considering the elastic zones contribution is given by equation 44:

$$P = \frac{P}{w} + P_{ei} + P_{ef} \tag{44}$$

For the first iteration in the iteration process, the deformed radius (R') is replaced with the regular roll radius (R) at all equations. With the value for (P) now calculated, it is then used in equation 21 to calculate the deformed roll radius. This new deformed roll radius is used to recalculate a new rolling load. The process is continued until the stop criterion is met.

2.3 Noncircular model

Newly studied mathematical models for extremely thin and hardened sheets show that the rolls undertake severe elastic deformation and the contact surface does not remain circular. As proposed by Le and Sutcliffe (2001), the first deformation at onset of contact is an elastic compression; when stresses have grown to such an extent that the yield condition is met, plastic deformation starts; as the strip speed is increasing, the slip condition prevails; a flat, sticking zone may occur under higher loads at the center; followed by a second plastic reduction zone - with slip. In all cases, the contact is bounded by a final elastic unloading zone which begins at the minimum thickness point x_d (Shigaki *et al*, 2015).

The formulation is derived from the work by Le and Sutcliffe (2001). Only a summary is given here. The material is elastic-plastic work-hardening. Following the Slab Method, strain and stresses do not vary in the thickness direction, they are independent of *y*. The balance of the forces applied to all the sides of the slab (Fig. 3 and 4) in the rolling direction writes:

$$h\frac{d\sigma_1}{dx} + (\sigma_1 + p)\frac{dh}{dx} + 2\tau_s = 0 \tag{45}$$

x is the coordinate in the rolling direction, *h* the strip thickness, σ_1 the tensile stress in the rolling direction, *p* the interface pressure and τ_s the shear stress.

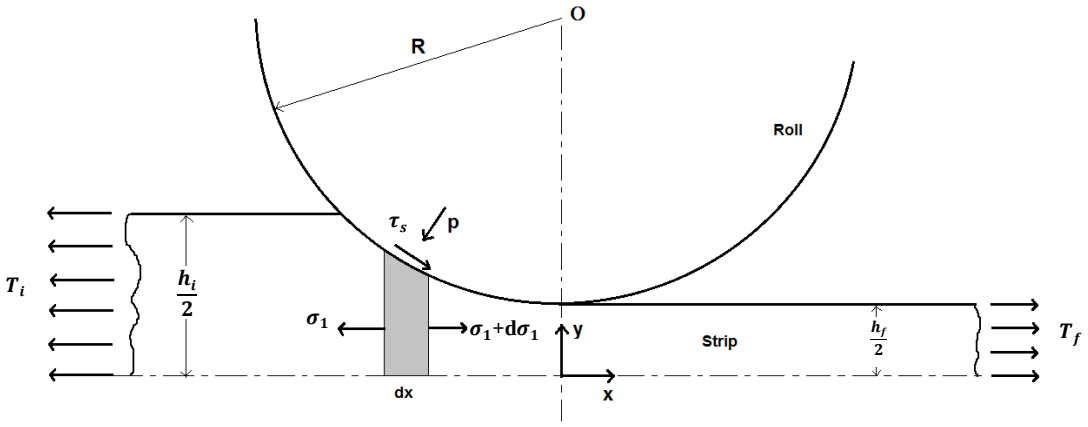

Figure 3 - Notations of the slab method.
Source: Adapted from Shigaki *et al*, (2015).

The equations governing the different zones are given next:

a) plastic slip zone: the equilibrium equation (45) is solved simultaneously with the elastic-plastic constitutive equations. A Tresca yield criterion is assumed: $p + \sigma_1 = S$ (*S* is the plane strain yield stress of the strip). Reporting into Eq. (45) gives:

$$\frac{dp}{dx} = \frac{S}{h}\frac{dh}{dx} + \frac{2\tau_s}{h} + \frac{dS}{dx} \tag{46}$$

The friction stress τ_s, wherever sliding is present, is given by:

$$\tau_s = \pm\mu p \tag{47}$$

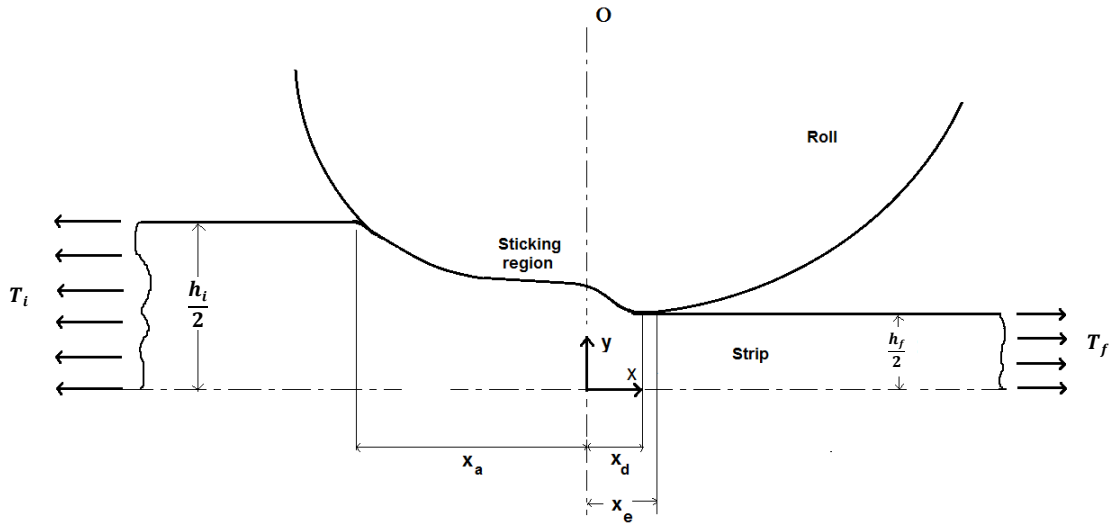

Figure 4 - The CPZ, Contained Plastic Zone, in the deformed contact arc.
Source: Adapted from Shigaki *et al*, (2015).

Where "+" stands for the backward slip at entry and the "-" for the forward slip at exit. The Coulomb friction coefficient μ is assumed constant.

In case regularization is applied, Eq. (47) is rewritten as:

$$\tau_s = \mu p . \frac{v_s}{\sqrt{v_s^2 + K_{reg}^2 . V_{roll}^2}} \tag{48}$$

V_{roll}, the work roll velocity, is introduced to non-dimensionalize the regularization coefficient (from now on termed K_{reg}). The slip velocity v_s is derived from volume conservation, neglecting elastic compressibility:

$$v_s = \left(\frac{h_n}{h_x} - 1\right) V_{roll} \tag{49}$$

Where h_n and h_x are the strip thickness at the neutral point and at point x, respectively.

b) elastic zones at entry and exit of the roll bite: strip / roll slip occurs. Following Le and Sutcliffe (2001), the elasticity and equilibrium equation are reprocessed:

$$\frac{dp}{dx} \cong -\frac{E_s^*}{h}\frac{dh}{dx} + \frac{v_s}{1 - v_s}\frac{2\tau_s}{h} \tag{50}$$

c) contained plastic zone (CPZ): the no-slip condition is used to calculate pressure gradient and shear stress for roll and strip. Equations (46) and (47) are replaced by:

$$\frac{dp}{dx} = -\frac{C_1 E_s^*}{h}\frac{dh}{dx} + C_1 \frac{1 - 2v_s}{1 - v_s}\frac{dS}{dx} \tag{51}$$

(52)

$$\tau_s = \frac{h}{2}\left[C_1 \frac{(1-2\nu_s)}{(1-\nu_s)} - 1\right]\frac{dS}{dx} - S\frac{dh}{dx} - \frac{C_1 E_s^*}{2}\frac{dh}{dx}$$

$$C_1 = \left[\frac{2-4\upsilon_s}{1-\upsilon_s} - \frac{(1-2\upsilon_R)}{(1-\upsilon_R)}\frac{E_s^*}{E_R^*}\right]^{-1} \tag{53}$$

In the cases addressed here (steel rolls and strip), $\nu_s = \nu_R$ (strip and roll Poisson's coefficient) and $E_s^* = E_R^*$ (plane strain Young's modulus for the strip and roll). Hence $C_1 = (1-\nu)/(1-2\nu) \approx 1.8$ so that Equations 51 and 52 give:

$$\frac{dp}{dx} = -\frac{C_1 E_s^*}{h}\frac{dh}{dx} + \frac{dS}{dx} \tag{54}$$

$$\tau_s = -\left(S + \frac{C_1 E_s^*}{2}\right)\frac{dh}{dx} \tag{55}$$

Finally, S is very small ($\approx 0.3\%$) compared with the other term of Eq. (55), hence:

$$q = -\left(\frac{C_1 E_s^*}{2}\right)\frac{dh}{dx} \tag{55b}$$

This slip-less zone begins where $\tau_s(x)$ (Eq. 55b) first crosses $\tau_s(x)$ for slipping condition (Eqs. 46-49). It ends at the second intersection point. This technique has been developed to forbid any increase of the local strip thickness inside the roll bite, as discussed above.

The system of equations is integrated by a 4th order Runge-Kutta method (RK4). Each zone is discretized into 3000 slabs (i.e. space integration steps).

The work roll deformation model is based on the Influence Function Method, based on the superposition principle. The influence coefficients used here were developed by Meindl (2001); Krimpelstätter (2007) used them for temper rolling. These influence functions are computed for a diametrically symmetric loading, not exactly what occurs in strip rolling: the work roll / back-up roll contact is shorter and undergoes higher contact stress than the strip / work roll contact. However, Saint-Venant's principle is exploited: the contact arc length is a few mm, much smaller than roll diameter (400 to 600 mm), so that only the resultant load at work roll / back-up roll contact needs to be exact, not its distribution.

Generally, four types of terms can be computed, relating orthoradial and radial stresses to radial and orthoradial displacements. Krimpelstätter (2007) claimed that orthoradial terms are necessary for temper-rolling (very small reduction, hence very local load on the roll). In the following, only the coefficients connecting the radial displacement to the radial load are used, a sufficient approximation for the large reduction cases investigated here.

Displacement is calculated on a roll fraction roughly twice as long as the arc of contact, divided into 200 intervals so that $\alpha = 2.7\ 10^{-4}$ radian.

Another interesting concept introduced by Wiklund and Sandberg (2002) was the use of the "flattening risk factor", β, calculated as below:

$$\beta = \frac{L}{h_i} \tag{56}$$

Where L is the contact arc length given by Eq. 12 and h_i is the sheet thickness at entry. The authors state that when the risk factor exceeds 10, severe roll flattening is expected (Lenard, 2007).

3 METHODOLOGY

Using a Matlab's programming language, both models were implemented, Bland and Ford (1948) (BF) and Alexander (1971) (AX). A cold rolling case was analyzed; it represents the last step when rolling thin metal sheets where the material is very work hardened. Only the friction coefficient was varied in this work. The main rolling parameters are stated in table 1 below:

Table 1 - Rolling cases parameters.

Parameters	Case 1	Case 2
Sheet thickness at entry (mm)	0.355	0.355
Sheet thickness at exit (mm)	0.252	0.252
Working roll radius (mm)	277.5	277.5
Material related coefficient AA	470.5	470.5
Material related coefficient BA	175.4	175.4
Material related coefficient CA	0.450	0.450
Material related coefficient DA	8.900	8.900
Material related coefficient EA	25.00	25.00
Material Young's modulus (GPa)	210.0	210.0
Working roll Young's modulus (GPa)	210.0	210.0
Material Poisson's coefficient	0.3	0.3
Working roll Poisson's coefficient	0.3	0.3
Friction coefficient	0.020268	0.0305
Front applied tension (MPa)	100.0	100.0
Back applied tension (MPa)	170.0	170.0
Accumulated strain	2.050	2.050

In both models (Alexander and Bland and Ford) the contact arc length was discretized in 1501 segments in order to solve the problem.

In the Bland and Ford's model the stopping criterion was that the relative error between the new found rolling load per sheet width and the last one should be smaller than 10^{-4}. In this model, Simpson's 1/3 rule was used to integrate the rolling load distribution over the contact arc length.

In the Alexander's model the stop criterion was that the relative error between the new found total rolling load per unit width and the last one should be smaller than 10^{-4}. In this model a fourth order Runge-Kutta routine is used to solve the first order differential equation and calculate the rolling load distribution over the contact arc length. Then, the Simpson's 1/3

rule is used to integrate the rolling load distribution and calculate the rolling load per unit width. Lastly the rolling load per unit width is added to the elastic zones contribution, hence the total rolling load per unit width is found.

The following parameters were chosen to be compared for both cases:

- Normal pressure distribution;
- Deformed roll surface and deformed radius value;
- Contact arc length;
- Total rolling load/width;

4 RESULTS

4.1 Normal pressure distribution

The friction hill, as it may be referred to, is the normal pressure distribution in the roll surface due to the contact pressure over the contact arc.

Figure 5 represents the normal pressure distribution over the contact arc for case 1, using Bland and Ford's, Alexander's and the Noncircular's model.

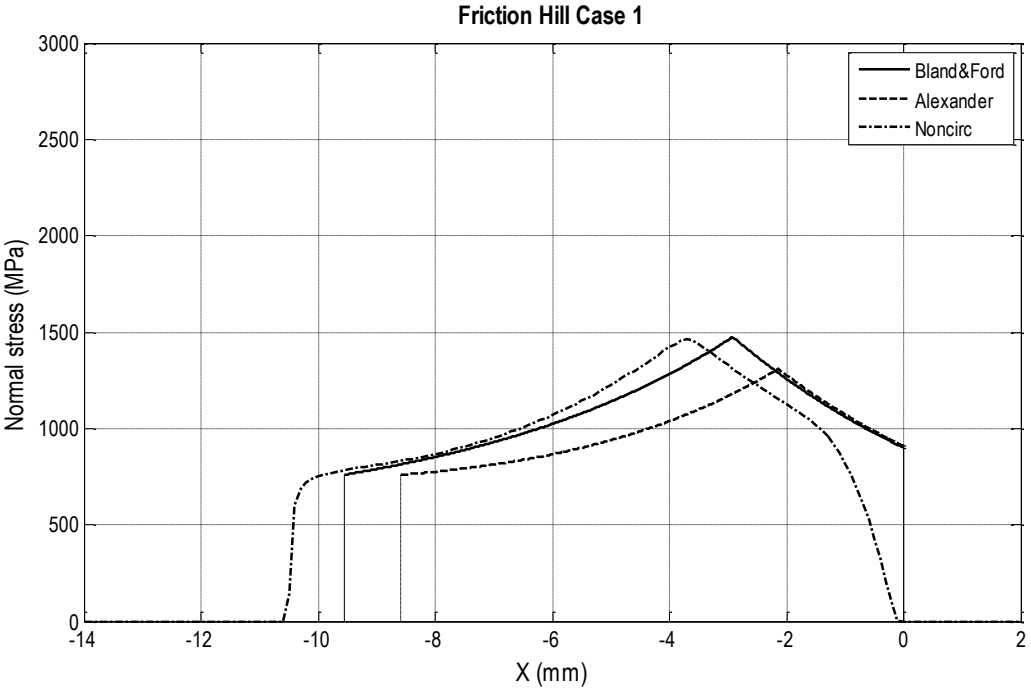

Figure 5 - Normal stress distribution over the contact arc for case 1.

Figure 6 represents the normal pressure distribution over the contact arc for case 2, using Bland and Ford, Alexander and the Noncircular models.

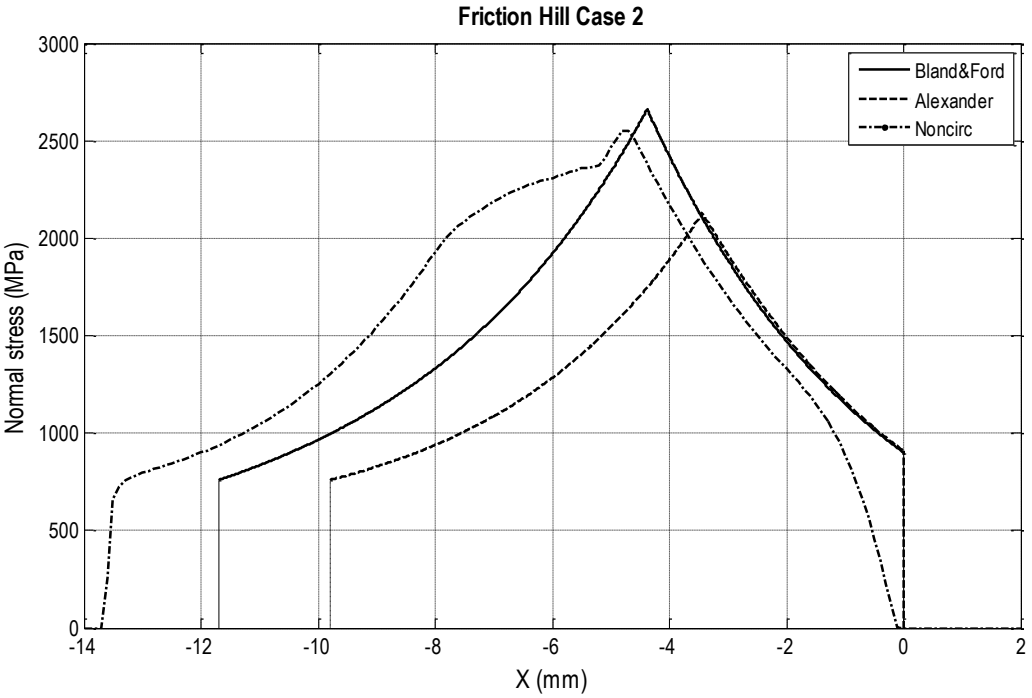

Figure 6 - Normal stress distribution over the contact arc for case 2.

4.2 Deformed roll surface and deformed roll radius

While Bland and Ford model's and Alexander's model consider the contact surface of the roll circular, the noncircular's model outputs the approximated deformed shape of the roll surface until the exit point at x = 0 for Case 1.

Figure 7 represents the deformed surfaces for the upper roll for the simulation of case 1 using the three models.

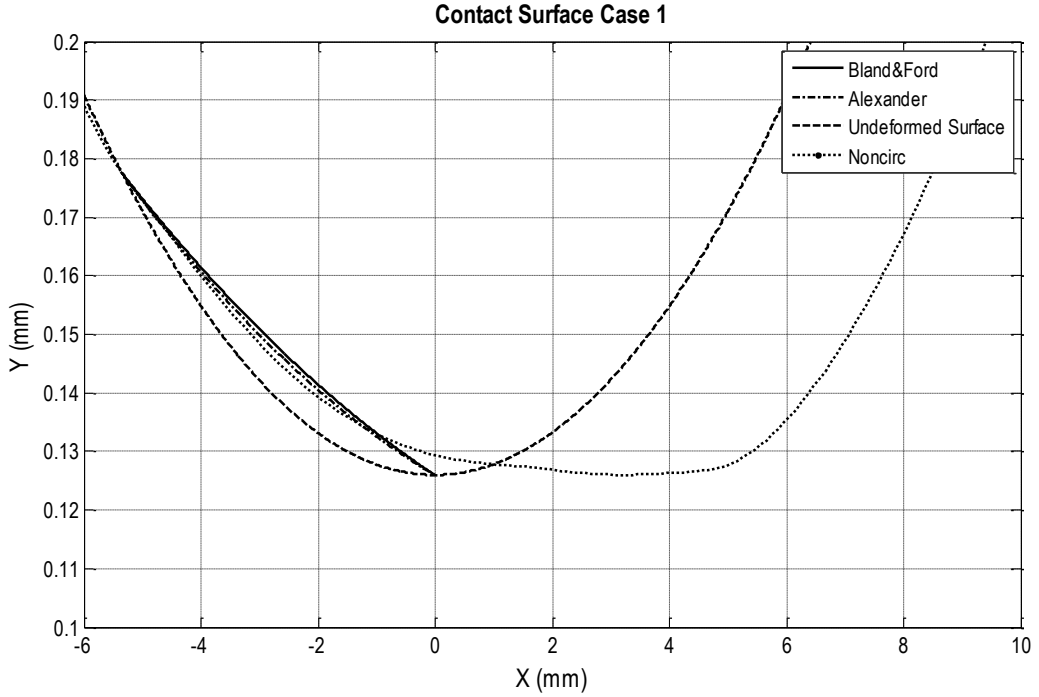

Figure 7 - Contact surface over the contact arc for case 1.

Figure 8 represents the deformed surfaces for the upper roll for the simulation of case 2 using the three models. In this case, the arc of contact calculated from Noncirc gives a length much longer than those from BF and Alexander.

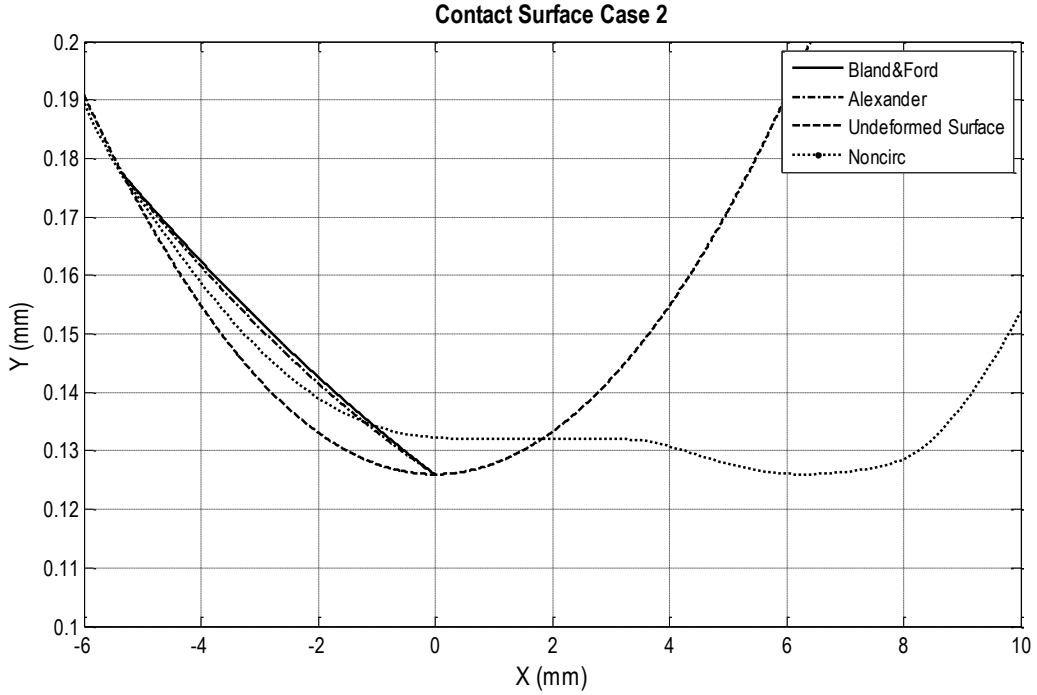

Figure 8 - Contact surface over the contact arc for case 2.

Table 2 refers to the values found for the deformed roll radius for both circular models.

Table 2 - Deformed roll radius.

Deformed roll radius (mm)	Case 1	Case 2
Bland and Ford	888.27	1330.07
Alexander	717.80	933.70

4.3 Contact arc length and total rolling load/width

For Bland and Ford's and Alexander models the contact arc length were estimated using Equation 12.

In another calculation, also using Equation 12, the deformed roll radius was used in order to estimate the contact arc length instead of the nominal roll radius.

The flattening risk factor was calculated using equation 56.

The total rolling load/width were calculated using Equations 14 and 44.

For the noncircular's model, the data was supplied by the co-author Shigaki.

Table 3 refers to the results for contact arc length and total rolling load/width for the three models.

Table 3 - Contact arc length and total rolling load/width.

Results	Case 1	Case 2
Bland and Ford		
Contact arc length (mm)	5.35	5.35
Contact arc length using deformed radius (mm)	9.57	11.70
Flattening risk factor	26.94	32.97
Total rolling load/width (N/mm)	10272.04	17702.40
Alexander		
Contact arc length (mm)	5.35	5.35
Contact arc length using deformed radius (mm)	8.60	9.81
Flattening risk factor	24.22	27.62
Total rolling load/width (N/mm)	9094.90	13679.32
Noncircular		
Contact arc length (mm)	10.60	13.70
Flattening risk factor	29.90	38.60
Total rolling load/width (N/mm)	10377.00	20622.00

5 CONCLUSION

Although it gives a good estimation, it is known that the friction hill is an unrealistic representation of actual roll pressures (Pietrzyk, 1991). Comparing the Bland and Ford's and Alexander's pressure distribution with the noncircular one for Cases 1 and 2, it can be seen that there are significant differences. It is known that noncircular models estimate better the load distribution over the contact arc for sheet thickness smaller than 0.4mm (Lenard, 2007), as is the case here. In their research, Wiklund and Sandberg (2002) found that the use of cylindrical roll deformation models is valid when the sheet thickness is thicker than 0.4mm. Therefore, noncircular roll deformation models are necessary when the thickness goes below that value, which results to severe roll flattening and leads to a flat contact region inside the roll gap, as it can be seen in figure 7 and 8. The flattening risk factor can be used as well.

It was pointed out in some detail by Roychoudhuri and Lenard (1984) that Hitchcock's formula does not predict the deformed roll shape very well. Figures 7 and 8 shows that there are expressive differences between the deformed roll surface predicted by Hitchcock's formula and the noncircular surface.

Comparing the values for the contact arc length, both models have shown good agreement with the noncircular values, but only when the deformed roll radius is used at Equation 12. Bland and Ford's model gives output closer to the results from noncircular model, though Lenard (2014) states that the original roll radius should be used for.

As the cases tested represent a severe rolling condition, as confirmed by the calculation of the flattening risk factor ($\beta>10$), the total rolling load/width found using both models may disagree with the literature and with the noncircular model used. The noncircular model is

considered a more precise and exact model due to its better contact surface deformation modeling, but has the shortcoming of not being suitable for online use (except for Dbouk et al., 2014). For controlling purposes, a Bland and Ford model may be used for most cases in order to give good results for rolling load, with some correction factors calculated from tuning the rolling mill with the computer model.

ACKNOWLEDGEMENT

We wish to thank CNPq, Proc. 488027/2013-6 and CEFET-MG for financial support for this research and FAPEMIG for the undergraduate student's research grant for Hugo L. F. Nascimento.

REFERENCES

Abdelkhalek, S., Montmitonnet, P., Legrand, N. & Buessler, P., 2011. Coupled approach for flatness prediction in cold rolling of thin strip. *International Journal of Mechanical Sciences,* v. 53, n. 9, p. 661-675.

Alexander, J. M., 1971. On the Theory of Rolling. *Proceedings of the Royal Society of London. Series A, Mathematical and Physical Sciences (1934-1990),* v. 326, n. 1567, p. 535-563.

Bland, D. R. & Ford, H., 1948. The calculation of roll-force and torque in cold strip rolling with tensions. *Proceedings of the Institution of Mechanical Engineers,* v. 159, p. 144.

Chen, S., Li, W. & Liu, X., 2014. Calculation of rolling pressure distribution and force based on improved Karman equation for hot strip mill. *International Journal of Mechanical Sciences,* v. 89, p. 256-263.

Dbouk, T., Montmitonnet, P., Suzuki, N., Takahama, Y. , Legrand, N. & Matsumoto, H., 2014. Advanced roll bite models for cold and temper rolling processes, *La Metalurgia Italiana*, v. 4, pp. 39-49.

Ford, H., Ellis, F. & Bland, D. R., 1951. Cold rolling with strip tension, Part I. A new approximate method of calculation and a comparison with other methods. *Journal of the Iron and Steel Institute,* v. 168, p. 57.

Freshwater, I. J., 1996. Simplified theories of flat rolling—I. The calculation of roll pressure, roll force and roll torque. *International Journal of Mechanical Sciences,* v. 38, n. 6, p. 633-648.

Grimble, M. J., Fuller, M. A. & Bryant, G. F., 1978. A noncircular arc roll force model for cold rolling. *International Journal for Numerical Methods in Engineering,* v. 12, p. 643-663.

Helman, H. & Cetlin, P. R., 2005. *Fundamentos da conformação mecânica dos metais.* 2 ed. São Paulo: Artliber Editora.

Krimpelstaetter, K., Hohenbichler, G., Finstermann, G. & Zeman, K., 2007. New noncircular arc skin pass model. *Ironmaking e Steelmaking,* v. 34, n. 4, p. 295-302.

Lenard, J. G., 2014. *Primer on Flat Rolling*. Elsevier Science. 2nd edition.

Montmitonnet, P., 2006. Hot and cold strip rolling processes. *Computer Methods in Applied Mechanics and Engineering,* v. 195, n. 48-49, p. 6604-6625.

Orowan, E., 1943. The calculation of roll pressure in hot and cold flat rolling. *Proceedings of the Institution of Mechanical Engineers*, v. 150, p. 140.

Pietrzyk, M. & Lenard, J. G., 1991. Thermal-Mechanical Modelling of the Flat Rolling Process. Springer. Verlag Berlin Heidelberg

Roberts, W. L., 1978. *Cold Rolling of Steel*. Taylor e Francis.

Shigaki, Y., Nakhoul, R. & Montmitonnet, P., 2015. Numerical treatments of slipping/no-slip zones in cold rolling of thin sheets with heavy roll deformation. *Lubricants,* v. 3, n. 2, p. 113.

Siebel, E., 1925. Kraft und materialflub bei der bildsamen formanderung. *Stahl Eisen,* v. 45, n. 37, p. 1563.

Sims, R. B., 1945. The calculation of the roll force and torque in hot rolling mills. *Proceedings of the Institution of Mechanical Engineers,* v. 168, p. 191-200.

Von Karman, T., 1925. Bietrag zur theorie des walzvorganges. *Zeitschrift für Angewandte Mathematik und Mechanik,* v. 5, p. 1563.

Wiklund, O. & Sandberg, F., 2002. *Chapter 15 - Modelling and Control of Temper Rolling and Skin Pass Rolling, In Metal Forming Science and Practice*, edited by J.G. Lenard,, Elsevier Science Ltd, Oxford, Pages 313-343, ISBN 9780080440248, http://dx.doi.org/10.1016/B978-008044024-8/50015-1.

Yang, Y. Y., Linkens, D. A. & Talamantes-Silva, J., 2004. Roll load prediction - Data collection, analysis and neural network modelling. *Journal of Materials Processing Technology,* v. 152, n. 3, p. 304-315.